

Solution speciation controls mercury isotope fractionation of Hg(II) sorption to goethite

Martin Jiskra, Jan Georg Wiederhold, Bernard Bourdon, and Ruben Kretzschmar

Environ. Sci. Technol., **Just Accepted Manuscript** • DOI: 10.1021/es3008112 • Publication Date (Web): 21 May 2012

Downloaded from <http://pubs.acs.org> on May 23, 2012

Just Accepted

“Just Accepted” manuscripts have been peer-reviewed and accepted for publication. They are posted online prior to technical editing, formatting for publication and author proofing. The American Chemical Society provides “Just Accepted” as a free service to the research community to expedite the dissemination of scientific material as soon as possible after acceptance. “Just Accepted” manuscripts appear in full in PDF format accompanied by an HTML abstract. “Just Accepted” manuscripts have been fully peer reviewed, but should not be considered the official version of record. They are accessible to all readers and citable by the Digital Object Identifier (DOI®). “Just Accepted” is an optional service offered to authors. Therefore, the “Just Accepted” Web site may not include all articles that will be published in the journal. After a manuscript is technically edited and formatted, it will be removed from the “Just Accepted” Web site and published as an ASAP article. Note that technical editing may introduce minor changes to the manuscript text and/or graphics which could affect content, and all legal disclaimers and ethical guidelines that apply to the journal pertain. ACS cannot be held responsible for errors or consequences arising from the use of information contained in these “Just Accepted” manuscripts.

Work that was subsequently accepted for publication in Environmental Science & Technology, copyright © American Chemical Society after peer review. To access the final edited and published work see:

<https://pubs.acs.org/doi/10.1021/es3008112>

1
2
3
4
5
6
7 1 Solution speciation controls mercury isotope
8
9
10
11 2 fractionation of Hg(II) sorption to goethite
12
13
14
15

16 3 *Martin Jiskra,^{†,‡} Jan G. Wiederhold,^{*,†,‡} Bernard Bourdon,^{‡,§} Ruben Kretzschmar[†]*
17
18

19 4 Institute of Biogeochemistry and Pollutant Dynamics, and Institute of Geochemistry and Petrology,
20
21
22 5 ETH Zurich, Switzerland
23
24
25 6

26
27
28 7 * Corresponding author e-mail: wiederhold@env.ethz.ch; phone: +41-44-6336008; fax: +41-44-6331118
29
30

31 8 † Institute of Biogeochemistry and Pollutant Dynamics, ETH Zurich, Switzerland
32
33

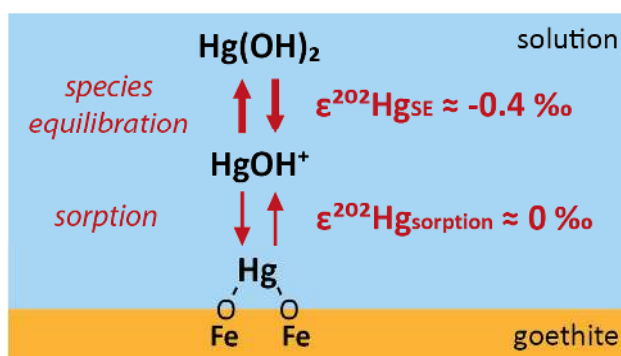
34 9 ‡ Institute of Geochemistry and Petrology, ETH Zurich, Switzerland
35
36

37 10 § Present address: Laboratoire de Géologie de Lyon, ENS Lyon, CNRS and UCBL, Lyon, France
38
39
40
41 11
42
43
44
45 12
46
47
48
49 13
50
51
52
53 14
54
55
56
57 15
58
59
60 16

17 ABSTRACT

18 The application of Hg isotope signatures as tracers for environmental Hg cycling requires the
19 determination of isotope fractionation factors and mechanisms for individual processes. Here, we
20 investigated Hg isotope fractionation of Hg(II) sorption to goethite in batch systems under different
21 experimental conditions. We observed a mass-dependent enrichment of light Hg isotopes on the goethite
22 surface relative to dissolved Hg ($\epsilon^{202}\text{Hg}$ of -0.30‰ to -0.44‰) which was independent of pH, chloride
23 and sulfate concentration, type of surface complex, and equilibration time. Based on previous theoretical
24 equilibrium fractionation factors, we propose that Hg isotope fractionation of Hg(II) sorption to goethite
25 is controlled by an equilibrium isotope effect between Hg(II) solution species, expressed on the mineral
26 surface by the adsorption of the cationic solution species. In contrast, the formation of outer-sphere
27 complexes and subsequent conformation changes to different inner-sphere complexes appeared to have
28 insignificant effects on the observed isotope fractionation. Our findings emphasize the importance of
29 solution speciation in metal isotope sorption studies and suggest that the dissolved Hg(II) pool in soils
30 and sediments, which is most mobile and bioavailable, should be isotopically heavy, as light Hg
31 isotopes are preferentially sequestered during binding to both mineral phases and natural organic matter.

32 TOC Art



Introduction

Soils worldwide contain a total pool of 1.15×10^6 tons of mercury (Hg) and represent the most important terrestrial sink for atmospherically deposited Hg from natural and anthropogenic sources.¹ Mercury in soils can be exported to aquatic environments, re-emitted as Hg^0 to the atmosphere, or methylated under anoxic conditions to form neurotoxic and bioaccumulating methyl-Hg.² However, the largest Hg pool in soils is bound to organic and mineral soil phases, where it is immobilized.¹ In organic topsoils, Hg is mainly bound to reduced organic sulfur groups,³ whereas in soils and sediments with low organic matter contents, mineral phases like Fe and other metal (oxyhydr)oxides and clay minerals play an important role as sorbents.^{4,5} In addition, Fe (oxyhydr)oxides form colloidal particles in natural aquatic and terrestrial environments and can thus act as carriers of sorbed metals such as Hg by colloidal transport.⁶

The fractionation of stable Hg isotopes in nature has gained much attention in recent years,^{7,8,9} as it provides a promising tracer for environmental Hg cycling. Mercury isotopes have been shown to exhibit mass-dependent fractionation (MDF) as well as mass-independent fractionation (MIF), caused by nuclear volume fractionation (NVF)¹⁰ or magnetic isotope effects (MIE)¹¹, together generating a multidimensional isotope signature. In order to apply stable Hg isotopes as a tool to understand the fate of Hg in the environment, one needs to understand Hg isotope fractionation factors and mechanisms of individual biogeochemical pathways. With this mechanistic information, it will be possible to deconvolute different sources and processes using measured stable Hg isotope ratios in natural samples. So far, Hg isotope fractionation has been studied experimentally for photoreduction of Hg^{2+} and methyl-Hg,^{12,13} abiotic and biotic methylation of Hg,^{14,15} abiotic and biotic reduction of Hg^{2+} ,^{16,17} photolytic and microbial methyl-Hg degradation,^{18,19} volatilization of elemental liquid Hg,^{20,21} and aqueous to gas phase transfer of elemental Hg.²² In a previous study, we investigated equilibrium isotope fractionation between dissolved Hg(II) species and thiol-bound Hg as a model system for sorption of Hg(II) to natural organic matter.²³ No data are available yet for stable isotope fractionation of Hg sorption to mineral phases. However, stable isotope fractionation during sorption to minerals has been described for other metals. Sorption studies for Cu(II),^{24,25} Zn(II),^{25,26} and Fe(II),^{27,28} to mineral phases (Fe- and Mn-

1
2
3 61 (oxyhydr)oxides) revealed that sorption was in most cases associated with an enrichment of heavy
4
5 62 isotopes on mineral surfaces relative to the dissolved phase. The observed isotope fractionation was
6
7
8 63 explained by the lower vibrational frequencies of the sorption complexes with heavy isotopes and thus a
9
10 64 lower zero-point energy compared with complexes with light isotopes.²⁹ In contrast, an isotope
11
12 65 fractionation towards light isotopes on the mineral surface for metals sorbing as cations has been
13
14
15 66 observed for some Zn experiments³⁰ and preliminary Cd data,³¹ a mechanistic interpretation is however
16
17 67 lacking. Mo(VI) and U(VI), both predominantly present in anionic form, showed a preferential sorption
18
19 68 of light isotopes to Mn-(oxyhydr)oxides.^{32,33} The interpretation of these isotope effects is still under
20
21
22 69 debate: in the case of U(VI), the isotope fractionation was attributed to a change in coordination
23
24 70 environment between the dissolved and sorbed phase.³³ For Mo(VI) it has been proposed that the
25
26 71 isotope fractionation is caused by an equilibrium isotope effect between different solution species,
27
28 72 where only the minor species is actively sorbing.^{34,35} However, a newer study postulates a fractionation
29
30
31 73 between the dissolved Mo and a polynuclear surface precipitate.³⁶
32

33 74 In this study we present the first data for Hg isotope fractionation during sorption processes to
34
35 75 mineral surfaces. Goethite (α -FeOOH) was chosen as sorbent because it is the most abundant iron
36
37 76 (oxyhydr)oxide in soils³⁷ and Hg(II) sorption to goethite has been studied both with macroscopic^{38,39}
38
39
40 77 and spectroscopic techniques.^{40,41} The objectives of this study were (i) to investigate stable Hg isotope
41
42 78 fractionation associated with sorption of Hg(II) to goethite under different environmentally relevant pH
43
44
45 79 conditions, chloride and sulfate concentrations, and after different equilibration times, and (ii) to
46
47 80 elucidate the mechanisms driving Hg isotope fractionation of sorption based on our experimental
48
49
50 81 results, previously presented surface complexation studies, and theoretical calculations for equilibrium
51
52 82 fractionation factors of Hg species.

53 83 **Experimental Section**

54 84 **Materials and reagents.** The goethite was synthesized following a standard method (preparation from
55
56 85 an alkaline system after Böhm, 1925) described in Schwertmann and Cornell⁴² and was already used
57
58
59
60 86 and characterized in previous studies.^{43,44} The structure of the synthesized goethite was confirmed by

1
2
3 87 X-ray diffraction (XRD) and a surface area of $38 \text{ m}^2 \text{ g}^{-1}$ was measured using the N_2 -BET method.⁴³ All
4
5 88 chemicals used in this study were analytical grade and used without further treatment, if not indicated
6
7
8 89 otherwise. A detailed list of reagents, chemical impurities, and preparation procedures is provided in the
9
10 90 Supporting Information (SI).

11
12 91 **Batch experiments.** Two types of sorption experiments were performed in batch reactors to assess the
13
14
15 92 Hg isotope fractionation at different fractions of the total Hg sorbed to goethite. In the pH series, the
16
17 93 sorbed fraction of Hg was varied by adjusting the suspension pH to values between 3.1 and 6, and in the
18
19 94 mercury-to-goethite-ratio (MGR) series, the ratio between total Hg and goethite was varied at constant
20
21
22 95 pH 7. Goethite (between 0.5 to 20 g L^{-1} , see Table 1) was added to acid-washed 30-mL Teflon
23
24 96 centrifuge tubes and was dispersed by ultrasonication in 20 mL matrix solution. The experiments at pH
25
26 97 7 were performed in a buffer solution containing 2.5 mM 3-morpholino-propanesulfonic acid (MOPS),
27
28 98 whereas pH-series were unbuffered. Experiments were conducted in the absence and presence of
29
30
31 99 chloride and sulfate, respectively, which influences the speciation of Hg(II) in solution and on the
32
33 100 surface.^{41,45} For chloride-bearing experiments, the solution matrix contained 0.5 mM NaCl, for sulfate-
34
35 101 bearing experiments, 0.95 M Na_2SO_4 was added, as listed in Table 1. The pH was adjusted by titration
36
37
38 102 with diluted HNO_3 or NaOH. Aliquots of a Hg(II)-nitrate stock solution were then added to the goethite
39
40 103 suspension to yield an initial Hg concentration of 5 to 25 μM and equilibrated during 18 h, 72 h, or
41
42 104 720 h on an end-over-end shaker at room temperature in the dark. To separate the sorbed and dissolved
43
44
45 105 pools, the equilibrated samples were centrifuged at 3000 rpm for 15 min. The supernatants were
46
47 106 decanted and filtered through 0.2- μm Nylon filters to obtain the dissolved pool. The goethite, containing
48
49 107 the sorbed Hg, was dissolved in 6 M HCl at 80°C . All samples were stabilized with 1 % BrCl (v/v) (0.2
50
51 108 M BrCl in $\text{HCl}_{\text{conc.}}$) and stored at 4°C prior to analysis.

52
53
54 109 **Analytical methods.** Hg concentrations were measured by cold vapor atomic fluorescence spectrometry
55
56 110 (CV-AFS, Millennium Merlin, PS Analytical, U.K.). Samples were diluted to 2.5 to 25 nM for
57
58
59 111 concentration measurements. Standards prepared in triplicate reproduced with $\pm 3.6 \%$ (2σ), which is
60
112 reported as the uncertainty of the concentration measurements. Hg isotope ratios were measured by cold

vapor generation (HGX-200, Cetac, Omaha, U.S.) coupled to a multicollector inductively-coupled plasma mass spectrometer (MC-ICPMS, Nu instruments; Wrexham, U.K.). In addition to standard bracketing, mass bias was corrected by Tl addition using a desolvating nebulizer. This method was previously described in detail²³ and further information is provided in the SI. All isotope ratios of samples and secondary standards were measured relative to NIST-3133, which was used as bracketing standard. We report Hg isotope data following the nomenclature suggested by Blum and Bergquist,⁴⁶ adapted to recent recommendations of IUPAC:⁴⁷

$$\delta^{202}\text{Hg}_{\text{NIST-3133}} = \frac{(^{202}\text{Hg}/^{198}\text{Hg})_{\text{sample}}}{(^{202}\text{Hg}/^{198}\text{Hg})_{\text{NIST-3133}}} - 1 \quad (1)$$

$$\Delta^{199}\text{Hg} = \delta^{199}\text{Hg} - (\delta^{202}\text{Hg} \times 0.2520) \quad (2)$$

The mass-independent fractionation, expressed here as $\Delta^{199}\text{Hg}$, represents the deviation of the isotope ratio from the mass dependent fractionation line, where 0.2520 was used as the kinetic mass dependent scaling factor for $\delta^{199}\text{Hg}$, calculated in analogous manner to $\delta^{202}\text{Hg}$ based on $^{199}\text{Hg}/^{198}\text{Hg}$. Please note that the use of the equilibrium mass dependent scaling factor (0.2539) would not alter our results in a significant manner and we decided to use the kinetic factor for reasons of consistency with the nomenclature used in field studies.⁴⁶ Our in-house standard (ETH Fluka) was regularly measured between samples and reproduced at $\delta^{202}\text{Hg}_{\text{NIST-3133}} = -1.38 \pm 0.09 \text{ ‰}$, $\Delta^{199}\text{Hg} = +0.08 \pm 0.03 \text{ ‰}$ (2σ , $n=16$). For the UM-Almadèn standard (provided by Joel Blum, University of Michigan), we obtained isotope ratios of $\delta^{202}\text{Hg}_{\text{NIST-3133}} = -0.55 \pm 0.02 \text{ ‰}$, $\Delta^{199}\text{Hg} = -0.02 \pm 0.05 \text{ ‰}$ (2σ , $n=4$), which is in excellent agreement with published values ($\delta^{202}\text{Hg}_{\text{NIST-3133}} = -0.54 \pm 0.08 \text{ ‰}$, $\Delta^{199}\text{Hg} = -0.01 \pm 0.05 \text{ ‰}$ (2σ , $n=4$)).¹² Multiple measurements of the Hg(II)-nitrate salt used in the sorption experiments resulted in values of $\delta^{202}\text{Hg}_{\text{NIST-3133}} = -0.69 \pm 0.09 \text{ ‰}$ and $\Delta^{199}\text{Hg} = +0.01 \pm 0.03 \text{ ‰}$ (2σ , $n=4$). The ETH Fluka in-house standard and Hg(II)-nitrate salt both reproduced with $\pm 0.09 \text{ ‰}$ (2σ) for $\delta^{202}\text{Hg}$ and $\pm 0.03 \text{ ‰}$ (2σ) for $\Delta^{199}\text{Hg}$, which is considered to be the analytical precision for all reported measurements. To simplify further data analysis and presentation, Hg isotope ratios of all experimental data are in the

1
2
3 137 following reported relative to the composition of the Hg(II)-nitrate salt used in all experiments,
4
5
6 138 representing the starting condition:

$$8 \quad \delta^{202}\text{Hg} = \delta^{202}\text{Hg}_{\text{NIST-3133}}^{\text{sample}} - \delta^{202}\text{Hg}_{\text{NIST-3133}}^{\text{Hg(II)-nitrate salt}} \quad (3)$$

10
11 140 The fractionation of Hg isotopes on the goethite surface relative to the solution is expressed as
12
13 141 enrichment factor ϵ for mass-dependent fractionation (MDF):

$$15 \quad \epsilon^{202}\text{Hg}_{\text{sorbed-dissolved}} = \delta^{202}\text{Hg}_{\text{sorbed}} - \delta^{202}\text{Hg}_{\text{dissolved}} \quad (4)$$

17
18 143 and as enrichment factor E for mass-independent fractionation (MIF):

$$20 \quad E^{199}\text{Hg} = \epsilon^{199}\text{Hg} - (\epsilon^{202}\text{Hg} \times 0.2520) \quad (5)$$

22 145 Calculating the enrichment factors ($\epsilon^{202}\text{Hg}$ and $E^{199}\text{Hg}$) as difference of the isotope signature between
23
24
25 146 the sorbed and the dissolved pool averaged over the number of batches in an experimental series ($n = 3$
26
27 147 to 5) allowed us to ensure mass balance criteria. The uncertainties of the enrichment factors, reported as
28
29 148 one standard deviation σ , were calculated from the error propagation of the difference calculation based
30
31
32 149 on the above reported analytical precision ($\pm 0.09 \text{ ‰}$ (2σ) for $\delta^{202}\text{Hg}$ and $\pm 0.03 \text{ ‰}$ (2σ) for $\Delta^{199}\text{Hg}$). All
33
34 150 statistical tests were performed based on a 95 % confidence level. Further details on data analysis, mass
35
36 151 balance criteria, error propagation, and statistical tests are provided in the SI.

38 152 **Results and Discussion**

40
41 153 **Sorption of Hg to goethite.** In accordance with previous studies,^{38,39,48} the sorption of Hg(II) to goethite
42
43 154 exhibited a strong pH-dependence characterized by a distinct increase of the sorbed fraction with
44
45 155 increasing pH; for instance, from 15 % at pH 3.6 to 64 % at pH 5.3 (Figure S2, Table S4a). Addition of
46
47
48 156 chloride resulted in a pronounced decrease in Hg sorption compared to the chloride-free series (Figures
49
50 157 S2 and S3), which is due to the formation of stable Hg(II)-chloro complexes in solution.⁴⁵ The variation
51
52 158 of the mercury-to-goethite ratio (MGR) at constant pH 7 resulted in Hg surface coverages between
53
54
55 159 0.025 and 0.30 $\mu\text{mol m}^{-2}$. In the MGR-sulfate series, Hg showed a slightly lower sorption affinity
56
57 160 compared to the series in the absence of chloride and sulfate (Figure S3). Comparing the experiments
58
59 161 with different equilibration times (18 h, 72 h, and 720 h), we observed an increase in the sorbed fraction
60

1
2
3 162 of about 10 to 17 % between 18 h and 720 h equilibration (Figure S4). Similar observations were
4
5
6 163 previously reported for a time series from 2 h up to 8 weeks with an increase in the Hg fraction sorbed
7
8 164 to goethite without any clear endpoint.⁴⁹ EXAFS spectroscopy on Hg(II) sorbed to goethite at a surface
9
10 165 coverage (Γ) of $0.4 \mu\text{mol m}^{-2}$ provided no evidence for surface precipitation of Hg.^{40,41} As the surface
11
12 166 coverage in our experiments never exceeded $0.3 \mu\text{mol m}^{-2}$, we conclude that surface precipitation is
13
14
15 167 unlikely and Hg was sorbed as outer-sphere and/or inner-sphere complexes.

16
17 168 **Stable Hg isotope fractionation.** In all experiments, Hg sorbed to goethite was found to be enriched in
18
19 169 light Hg isotopes. Figure 1a displays the $\delta^{202}\text{Hg}$ isotope signature as a function of the fraction of total
20
21 170 Hg which was sorbed to goethite in the experimental series with no chloride and variable pH (pH series;
22
23
24 171 Table 1) and for an experimental series with varying mercury-to-goethite-ratio (MGR-72h series). Both
25
26 172 data sets exhibited an increase of $\delta^{202}\text{Hg}$ in the dissolved phase with increasing fraction of sorbed Hg.
27
28 173 The sorbed pool was correspondingly enriched in light Hg isotopes, as indicated by negative $\delta^{202}\text{Hg}$
29
30
31 174 values. The $\delta^{202}\text{Hg}$ signatures of the sorbed and dissolved Hg pools in the presence of 0.5 mM chloride
32
33 175 followed the same trends (Figure 1b). The enrichment factors $\epsilon^{202}\text{Hg}$, calculated from the difference
34
35 176 between the sorbed and dissolved $\delta^{202}\text{Hg}$ averaged over the number of batches in one experimental
36
37
38 177 series ($n = 3$ to 5), fell in a narrow range between $-0.30 \pm 0.04 \text{‰}$ and $-0.44 \pm 0.04 \text{‰}$ (Table 1). A
39
40 178 statistical test comparing the determined enrichment factors ($\epsilon^{202}\text{Hg}$, see SI) of the MGR-72h series in
41
42
43 179 the absence of chloride and the MGR-Cl series with 0.5 mM Cl^- revealed no significant differences.
44
45 180 Furthermore, the isotopic results of the two approaches used to vary the fraction of sorbed Hg (pH and
46
47 181 MGR series) were not significantly different from each other, both in the absence of chloride and with
48
49
50 182 0.5 mM Cl^- . Figure 2 shows the comparison between the experimental series with 0.95 M sulfate
51
52 183 (MGR-sulfate) and with no sulfate (MGR-72h). The enrichment factors for the MGR-sulfate and for the
53
54 184 MGR-72h series (see Table 1) were not significantly different from each other. Figure 3 shows a time
55
56 185 series of Hg(II) sorption to goethite with equilibration times of 18 h, 72 h, and 720 h. Even though there
57
58
59 186 was a significant increase in the fraction of sorbed Hg with time (Figure S4), the comparison of the time
60
187 series revealed no statistically significant difference between their enrichment factors ($\epsilon^{202}\text{Hg}$).

1
2
3
4
5
6
7
8
9
10
11
12
13
14
15
16
17
18
19
20
21
22
23
24
25
26
27
28
29
30
31
32
33
34
35
36
37
38
39
40
41
42
43
44
45
46
47
48
49
50
51
52
53
54
55
56
57
58
59
60

188 Therefore, although the adsorption of Hg was continuing, we observed no dependence of the Hg isotope
189 fractionation on equilibration time. The comparison of two alternative model approaches did not yield
190 conclusive results concerning the reversibility of the sorption process (see SI). None of the experimental
191 series showed mass independent fractionation expressed by $E^{199}\text{Hg}$ being significantly different from
192 zero (Figure 4b, Table 1, Table S2).

Table 1. Parameters of the experimental series: Number of batches in experimental series (n), amount of goethite (g L^{-1}), initial Hg concentration (Hg) in μM , pH, solution matrix with MOPS (2.5 mM), SO_4^{2-} (0.95 M) and Cl^- (0.5 mM), equilibration time (t_{eq}) in h, expected dominating Hg(II) surface complex with b for bidentate and m for monodentate, and isotopic enrichment factors of stable Hg isotopes on the goethite surface relative to the solution for mass-dependent fractionation ($\epsilon^{202}\text{Hg}$) and mass-independent fractionation ($E^{199}\text{Hg}$) with 1σ uncertainties (see SI for details). Each experimental series was performed with different fractions of total Hg sorbed, which was varied by different mercury-to-goethite-ratio (MGR series) or by different pH (pH series).

series	n	goethite (g L^{-1})	Hg (μM)	pH	solution matrix	t_{eq} (h)	Hg(II) surface complex	$\epsilon^{202}\text{Hg}$ (‰)	σ (‰)	$E^{199}\text{Hg}$ (‰)	σ (‰)
pH	5	5	5	3.1 - 6	-	72	$b^{50,40}$	-0.37	0.03	0.03	0.011
MGR-18h	4	0.5 - 20	25	7	MOPS	18	$b^{50,40}$	-0.36	0.03	-0.02	0.013
MGR-72h	4	0.5 - 20	25	7	MOPS	72	$b^{50,40}$	-0.32	0.03	-0.02	0.013
MGR-720h	3	0.5 - 9	25	7	MOPS	720	$b^{50,40}$	-0.42	0.04	-0.03	0.015
MGR-sulfate	3	0.5 - 9	25	7	MOPS, SO_4^{2-}	72	m^{41}	-0.30	0.04	0.01	0.015
pH-Cl	3	5	5	5 - 6	Cl^-	72	m^{41}	-0.32	0.04	0.00	0.015
MGR-Cl	3	0.5 - 9	10	7	MOPS, Cl^-	72	m^{41}	-0.44	0.04	-0.03	0.015

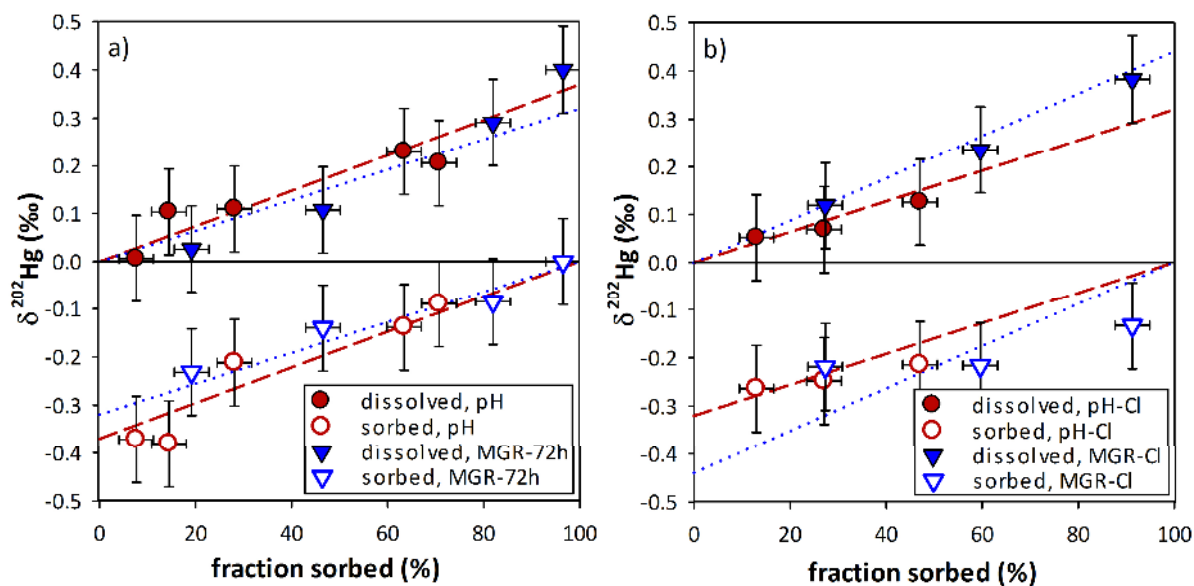


Figure 1. $\delta^{202}\text{Hg}$ of sorbed (open symbols) and dissolved (closed symbols) pool as a function of the Hg-fraction sorbed (in %). Experiments in the absence of chloride (a) and with 0.5 mM chloride (b) performed with 72 h equilibration time. The sorbed fraction was varied by changing the pH (pH and pH-Cl series) and by changing the mercury-to-goethite ratio (MGR-72h and MGR-Cl series). The equilibrium fractionation lines, derived from the calculated enrichment factors (see Table 1), are shown as dotted lines for the MGR series and dashed lines for the pH series.

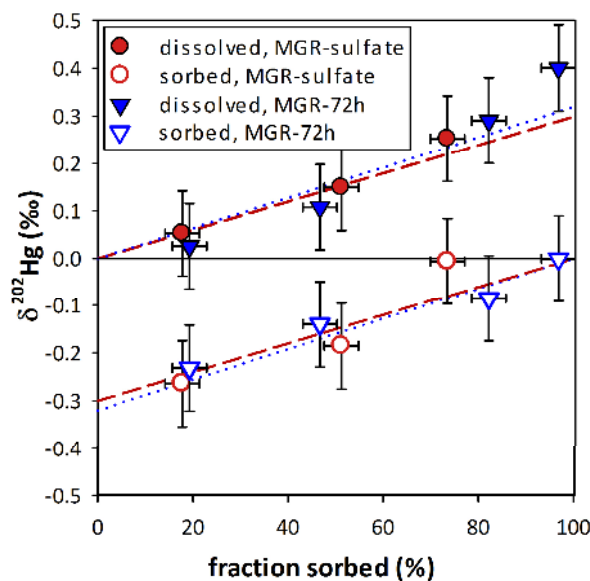


Figure 2. $\delta^{202}\text{Hg}$ of sorbed (open symbols) and dissolved (closed symbols) pool as function of fraction sorbed (in %). Experiments were performed with 0.95 M sulfate (circles, MGR-sulfate series) and in the absence of sulfate (triangles, MGR-72h series). The equilibrium fractionation lines, derived from the calculated enrichment factors, are shown as dashed lines for the MGR-sulfate series and dotted lines for the MGR-72h series without sulfate (see Table 1).

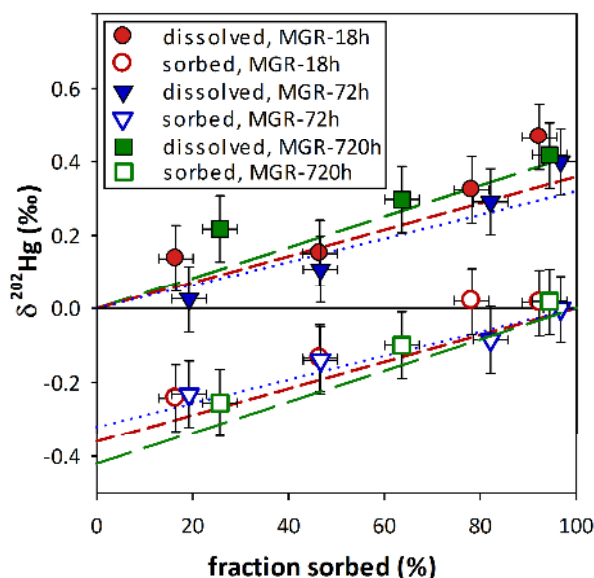
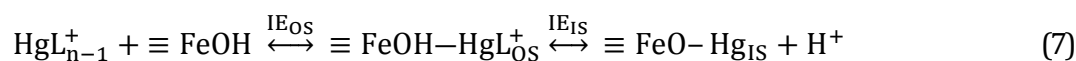


Figure 3. Hg isotope fractionation during sorption of Hg(II) to goethite as a function of equilibration time (18 h, 72 h, and 720 h, see Table 1). $\delta^{202}\text{Hg}$ of sorbed (open symbols) and dissolved (closed symbols) pool as function of fraction sorbed (in %). The equilibrium fractionation lines, derived from the calculated enrichment factors, are shown as short-dashed line for the MGR-18h series, as dotted lines for the MGR-72h series, and as long-dashed lined for the MGR-720h series (see Table 1).

Possible Hg isotope fractionation mechanisms. Previous studies identified the cationic Hg(II) species (HgOH^+ and HgCl^+) as the sorption active solution species as discussed further below.^{39,51} Following this, the sorption of Hg(II) to a mineral surface, in this case goethite ($\alpha\text{-FeOOH}$), can be described by the following reaction steps, which all might be potentially associated with an isotopic enrichment (IE):



Neutral dissolved Hg(II) species (HgL_n) dissociate to the cationic Hg(II) species (HgL_{n-1}^+) and the ligand (L^- , in our experiments OH^- or Cl^-). This species equilibration (SE) in solution might be associated with an equilibrium isotope effect (IE_{SE}). The sorption active Hg(II) cationic species (HgL_{n-1}^+) adsorbs to the goethite surface to form an outer-sphere complex ($\equiv \text{FeOH}-\text{HgL}_{\text{OS}}^+$) followed by the dehydration of the outer-sphere complex and a deprotonation of the goethite surface hydroxyl

1
2
3 236 group to form an inner-sphere complex ($\equiv \text{FeO}-\text{Hg}_{\text{IS}}$). The conformation change between the bonding
4
5
6 237 environment of the Hg(II) cation in solution and the outer-sphere complex could potentially cause an
7
8 238 isotopic enrichment (IE_{OS}), as well as the conformation change between the outer-sphere complex and
9
10 239 the inner-sphere complex during dehydration (IE_{IS}).
11

12 **Isotope fractionation during species equilibration in solution (IE_{SE}).** Species equilibration under the
13 240
14 experimental conditions presented here usually involves hydroxide as ligand and can be therefore
15 241
16 denoted for the most part as hydrolysis, with the exception of the dissociation of HgCl_2 , where chloride
17 242
18 is the leaving ligand. Based on the observed strong correlation between metal's first hydrolysis constant
19 243
20 and the surface complexation constant for metal sorption to mineral surfaces, the concept of hydrolysis
21
22 244 as first reaction step in the adsorption of Hg(II) to goethite was established.⁵² Following this, the
23
24 245 adsorption of Hg(II) to mineral phases was successfully modeled by the solution concentration of
25
26 246 HgOH^+ and HgCl^+ in the absence and presence of chloride, respectively, which were considered as the
27
28 247 sorption active species.^{39,51} Based on calculations performed using Visual MINTEQ⁵³ (database
29
30 NIST 46.7), in the absence of Cl^- and at pH 7, HgOH^+ occurs with an abundance of 0.06 % and all the
31 248
32 remaining Hg is present as $\text{Hg}(\text{OH})_2$. With 0.5 mM Cl^- at pH 7, HgCl^+ is present with 0.006 % and the
33 249
34 main solution species are HgClOH^0 (49.6 %), $\text{Hg}(\text{OH})_2^0$ (37.0 %), and HgCl_2^0 (13.4 %). It is important
35
36 250 to consider that after the removal of cationic species from solution by adsorption to surfaces, a re-
37
38 251 equilibration takes place which replenishes the small stock of cationic species by dissociation of the
39
40 252 dominant neutral Hg(II) species, which is very fast with a dehydration rate constant (k_w) for Hg(II) of
41
42 253 $9.3 \times 10^{10} \text{ s}^{-1}$.⁵⁴ Thus, the small pool size of the cationic Hg(II) species in solution does not preclude that
43
44 254 adsorption of larger amounts of Hg(II) to surfaces can proceed via the positively charged species which
45
46 exhibit a higher affinity for surface binding. Based on this fast equilibration between cationic and
47 255
48 neutral Hg species, an equilibrium isotope effect between those species can be transferred to the goethite
49
50 256 surface as the low abundance cations interact dominantly with the mineral surface.
51
52 257

53
54 258 **Calculated predictions of MDF and NVF.** We calculated the isotopic enrichment factor of cationic
55
56 259 species relevant in our experiments based on theoretical equilibrium isotope fractionation factors for
57
58
59 260
60
261

individual Hg species relative to elemental Hg vapor (calculated in gas phase) published by Wiederhold et al.²³ The equilibrium enrichment factors consist of a mass-dependent fractionation (MDF) component based on density functional theory and a nuclear volume fractionation (NVF) component based on relativistic Dirac-Coulomb calculations following the work of Schauble.¹⁰ The sum of the MDF and NVF component resulted in the predicted isotopic enrichment factor for each Hg species (MDF + NVF). Based on the assumption that $1000\ln\beta^{202-198} \approx \epsilon^{202}\text{Hg}$, the enrichment factor of the cationic species $\epsilon^{202}\text{Hg}_{\text{cat}}$ (HgOH^+ or HgCl^+) was calculated from the difference between the $1000\ln\beta_{\text{cat}}^{202-198}$ of the cationic species and the average of the $1000\ln\beta_{n_i}^{202-198}$ of the neutral species n_i , where f_{n_i} is their relative abundance.

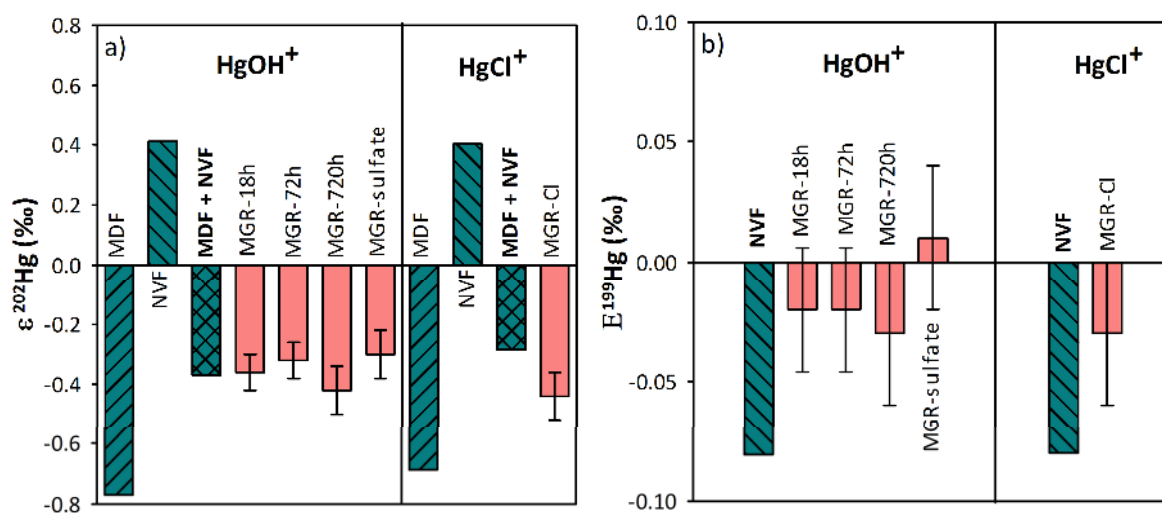
$$\epsilon^{202}\text{Hg}_{\text{cat}} = 1000\ln\beta_{\text{cat}}^{202-198} - \sum_i (f_{n_i} \times 1000\ln\beta_{n_i}^{202-198}) \quad (8)$$

NVF is related to the nuclear charge radii of the Hg isotopes which do not scale linearly with mass, therefore, NVF is associated with mass independent fractionation (MIF). The expected mass independent enrichment in $E^{199}\text{Hg}$ is calculated from the cationic enrichment factor of the nuclear volume component ($\epsilon^{202}\text{Hg}_{\text{NVF}}$) using the scaling factors of $^{199/198}\text{Hg}$ relative to $^{202/198}\text{Hg}$,²³ where SF_{MDF} is the kinetic mass dependent scaling factor of 0.252 and SF_{NVF} is the nuclear volume scaling factor of 0.0525 using nuclear charge radii from Landolt-Boernstein.⁵⁵

$$E^{199}\text{Hg} = (\epsilon^{202}\text{Hg}_{\text{NVF}} \times \text{SF}_{\text{NVF}}) - (\epsilon^{202}\text{Hg}_{\text{NVF}} \times \text{SF}_{\text{MDF}}) \quad (9)$$

Figure 4a shows the calculated Hg isotope enrichment factor of the cationic species HgOH^+ and HgCl^+ relative to the main solution species for the experimental series at pH 7. The 95 % confidence interval for all experimental series at pH 7 in the absence of chloride overlapped with the calculated enrichment factor (MDF+NVF) for HgOH^+ ($\epsilon^{202}\text{Hg} = -0.37 \text{ ‰}$). The calculated enrichment factor for HgCl^+ ($\epsilon^{202}\text{Hg} = -0.28 \text{ ‰}$), although not within the 95 % confidence interval of the chloride experiment (-0.36 ‰ to -0.52 ‰), was still in reasonable agreement with the experimental series. The NVF component of the calculations predicts a MIF of -0.08 ‰ in $E^{199}\text{Hg}$ both for the HgOH^+ and the HgCl^+ experiments, as illustrated by the NVF values in Figure 4b. However, none of the experimental series

1
2
3 287 showed any mass independent fractionation expressed by $E^{199}\text{Hg}$ being statistically different from zero
4
5
6 288 (Figure 4b, Table 1, Table S2). This discrepancy between the experimental findings and the theoretical
7
8 289 calculations for the Hg species is not yet fully understood. We can only speculate that there might be a
9
10 290 certain overestimation of the NVF component or the resulting extent of MIF in the calculations. Errors
11
12 291 on the species calculations might result from uncertainties of input parameters (nuclear charge radii), the
13
14 292 neglected influence of solvation effects, or the adequacy of the model; a quantification of these errors
15
16 293 however was not feasible (see SI of Wiederhold et al.²³ for detailed discussion on errors). The species
17
18 294 calculations for lower pH are not shown here, but they were in qualitative agreement with the results at
19
20 295 pH 7, although there are large uncertainties due to a lack of calculated $1000\ln\beta^{202-198}$ values for some
21
22 296 species present at lower pH (e.g., Hg^{2+}).
23
24
25
26



27
28
29
30
31
32
33
34
35
36
37
38
39
40
41
42
43
44 297
45
46 298 **Figure 4.** Calculated isotopic enrichment factors ($\epsilon^{202}\text{Hg}$ and $E^{199}\text{Hg}$) of cationic Hg species relative to
47
48 the dominant solution species at pH 7 are plotted as hatched bars.²³ In the absence of chloride the
49 299 isotopic fractionation was calculated for HgOH^+ , in the presence of chloride for HgCl^+ . The calculations
50
51 300 include two components from mass-dependent fractionation (MDF) and nuclear volume fractionation
52
53 301 (NVF). The sum of these results is the expected net effect (MDF+NVF). Plain bars represent
54
55 302 experimental enrichment factors (a: $\epsilon^{202}\text{Hg}$ for MDF, b: $E^{199}\text{Hg}$ for MIF, Table 1) of the Hg pool sorbed
56
57 303 to goethite relative to dissolved Hg.
58
59
60 304

1
2
3 305 **Isotope fractionation during surface complex formation (IE_{OS} , IE_{IS}).** As mentioned above, the
4
5 306 change in conformation between the dissolved Hg species and the sorption complexes (outer-sphere and
6
7 inner-sphere complex) could cause isotope fractionation as proposed in the example of Mo and U.^{32,33}
8 307
9
10 308 There are no calculations of enrichment factors for surface bound Hg species available and an
11
12 309 assessment of potentially different Hg isotope signatures of outer-sphere and inner-sphere complexes
13
14 was not possible, as only total sorbed Hg was measured. However, previous studies have identified
15 310
16 different types of inner-sphere surface complexes for different experimental conditions presented here.
17 311
18 Hg(II) sorbed to goethite forms bidentate inner-sphere complexes over the entire pH range investigated,
19 312
20 as shown by extended X-ray absorption fine structure (EXAFS) spectroscopy.^{40,50} High sulfate
21 313
22 concentrations (~1 M) were found to trigger the formation of ternary monodentate complexes
23 314
24 ($\equiv\text{Fe-O-Hg-SO}_4$),⁴¹ whereas the solution speciation of Hg is not significantly altered by sulfate addition.
25 315
26 Calculations with stability constants using Visual MINTEQ and literature data⁴⁵ predicted a $>10^6$ times
27 316
28 lower abundance of HgSO_4 and $\text{Hg}(\text{SO}_4)_2^{2-}$ compared to the predominant $\text{Hg}(\text{OH})_2$ species (over
29 317
30 99.99 % at pH 7), which was in agreement with previous calculations.⁴¹ There was no statistical
31 318
32 difference between Hg isotope fractionation of Hg(II) sorption to goethite in systems expected to form
33 319
34 bidentate surface complexes (MGR-72h series, Figure 2) and monodentate complexes (MGR-sulfate
35 320
36 series, Figure 2), which indicates that the conformation of inner-sphere complexes (IE_{IS}) does not
37 321
38 significantly influence the Hg isotope fractionation. This finding is supported by the experiments in the
39 322
40 presence of chloride, as the Hg isotope enrichment did not significantly vary compared with the absence
41 323
42 of Cl⁻, although a change in surface complexation towards ternary monodentate inner-sphere complexes
43 324
44 ($\equiv\text{Fe-O-Hg-Cl}$) was expected based on previous studies.^{41,56}
45 325
46
47
48
49
50

51
52 326 **Control of Hg isotope fractionation.** The measured isotopic enrichment between the sorbed and
53
54 dissolved pool can be expressed as a function of the isotopic enrichment of the cationic species during
55 327
56 equilibration in solution ($\epsilon^{202}\text{Hg}_{SE}$) and the isotopic enrichment during sorption of the cationic species
57 328
58 ($\epsilon^{202}\text{Hg}_{\text{sorption}}$) (derivation shown in SI):
59 329
60

$$\varepsilon^{202}\text{Hg}_{\text{sorbed-dissolved}} = \varepsilon^{202}\text{Hg}_{\text{sorption}} + (1 - f_{\text{cat}}) \times \varepsilon^{202}\text{Hg}_{\text{SE}} \quad (10)$$

The scaling term representing the relative fraction of cationic species ($1-f_{\text{cat}}$) was close to one in both experimental series (MGR-72h and MGR-Cl) as the cationic species occurred at very low abundances at pH 7 ($f_{\text{cat}(\text{HgOH}^+)} = 0.06 \%$, $f_{\text{cat}(\text{HgCl}^+)} = 0.006 \%$). As shown in Figure 4, the observed isotope fractionation between the sorbed and dissolved Hg-pool ($\varepsilon^{202}\text{Hg}_{\text{sorbed-dissolved}}$) is in good agreement with the predicted isotope enrichment of the cationic species during species equilibration ($\varepsilon^{202}\text{Hg}_{\text{SE}}$). Therefore, we conclude that the isotope fractionation of Hg(II) sorption ($\varepsilon^{202}\text{Hg}_{\text{sorbed-dissolved}}$) is controlled by an equilibrium isotope effect between Hg(II) solution species, expressed on the goethite surface by the adsorption of the cationic solution species. The isotopic fractionation during sorption of the cationic species ($\varepsilon^{202}\text{Hg}_{\text{sorption}}$), consisting of possible effects during conformation change between the cationic solution species and the outer-sphere complex (IE_{OS}) as well as during the dehydration of the outer-sphere complex to form an inner-sphere complex (IE_{IS}), appear to have an insignificant contribution. This is supported by the fact that the isotopic enrichment factors for experimental conditions forming monodentate inner-sphere complexes (MGR-sulfate and MGR-Cl series) were statistically indistinguishable from experiments forming bidentate complexes (e.g., MGR-72 h series). In addition, the finding that the observed isotope effect was insensitive to equilibration time provided further evidence that the different reaction steps at the mineral surface, some of which are expected to exhibit much slower kinetics compared with species equilibration in solution and thus explaining why the sorption had not yet reached a maximum, did not exert an important influence of the Hg isotope distribution in our system. Figure 5 shows the proposed schematic overview of the reaction steps involved in the sorption of Hg(II) to goethite and their associated Hg isotope enrichment factors for the example of HgOH^+ sorption.

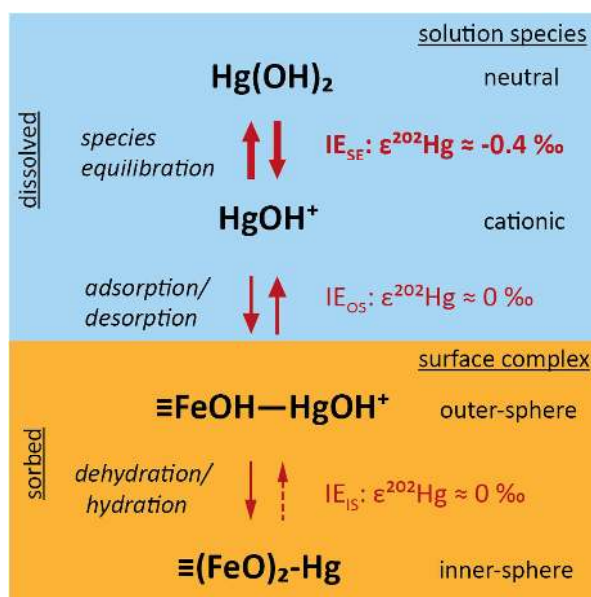


Figure 5. Proposed reaction scheme controlling Hg isotope fractionation of Hg(II) sorption to goethite.

The equilibrium isotope effect between Hg(II) solution species is transferred to the goethite surface through the sorption active cationic species which are isotopically lighter than the neutral solution species. Subsequent conformation changes between dissolved species and outer-sphere complexes as well as during dehydration to form inner-sphere complexes appear to have an insignificant effect on the overall isotopic fractionation.

Implications for other metal isotope and surface complexation studies.

We think that the detailed mechanistic insights provided by this study will have implications for other metal isotope systems as well as for the general understanding of metal sorption processes to mineral surfaces. On the one hand, the postulated importance of equilibrium isotope fractionation during hydrolysis, or in more general terms equilibration of solution species which are involved to a different extent in sorption processes, may influence the isotope fractionation during sorption for other metals as well. Apart from Hg(II), the correlation between the metal's hydrolysis constant and the metal's surface complexation constant was shown for other metal cations (Ag^+ , Pb^{2+} , Cd^{2+} , Zn^{2+} , Co^{2+} , Cu^{2+} , Ni^{2+}),^{52,57} most of which possess several stable isotopes. Theoretical investigations of stable isotope fractionation between solution species were recently published for some metal isotope systems (e.g., Ni, Zn).^{58,59,60} A comparison with experimental data for metal isotope fractionation during sorption to a mineral phase

1
2
3 370 could potentially help in further identifying the mechanisms causing metal isotope fractionation for
4
5
6 371 these elements too and may provide further validation for the concept presented here. On the other hand,
7
8 372 stable isotope fractionation during sorption of other metals could also be influenced to a larger extent by
9
10 373 surface reactions depending on the relative importance of the factors and processes described in
11
12 374 equation 10, which could be different compared with the specific example of Hg(II) presented here. In
13
14
15 375 the context of surface complexation, this study demonstrates that stable isotope fractionation studies can
16
17 376 offer new insights into reaction mechanisms at mineral surfaces and provide further evidence for
18
19 377 existing surface complexation models.
20

21
22 378 **Implications for stable Hg isotopes as environmental tracer.** The observed MDF and the absence of
23
24 379 MIF during sorption of Hg(II) to goethite have been shown to be constant over a range of pH, as well as
25
26 380 chloride and sulfate concentrations which trigger the formation of different surface complexes.
27
28
29 381 Although the experiments were performed at higher concentrations than generally found in the
30
31 382 environment, the constant Hg isotope fractionation over a large range of surface coverages (between
32
33 383 0.002 and 0.3 $\mu\text{mol m}^{-2}$) allows the transfer of our results to environmental systems, as there is no
34
35
36 384 indication of a concentration dependence of the determined enrichment factors. This lack of dependence
37
38 385 upon concentration, chemical conditions, and equilibration time will facilitate the interpretation of
39
40 386 natural Hg isotope fractionation in soils and sediments driven by sorption processes.
41

42
43 387 Previous field studies have reported systematic differences between Hg isotope compositions of
44
45 388 different environmental compartments or Hg pools. For instance, a consistent offset of $0.60 \pm 0.16 \text{ ‰}$
46
47 389 between fish and sediment samples ($\delta^{202}\text{Hg}$, corrected for photochemical effects deduced from MIF)
48
49
50 390 was reported from the San Francisco Bay, USA⁶¹ and water leachates were found to be enriched by 0.70
51
52 391 $\pm 0.13 \text{ ‰}$ in $\delta^{202}\text{Hg}$ compared with soil samples from a mining site in China.⁶² We suggest, based on the
53
54 392 results of this study as well as the previously published work on Hg(II)-thiol binding,²³ that sorption
55
56 393 processes may be at least partially responsible for these observed systematic offsets and influence the
57
58
59 394 isotope signature of natural Hg pools to a significant extent. Sorption of Hg(II) to goethite as well as
60
395 sorption of Hg(II) to thiol groups,²³ studied as a model system for binding to natural organic matter,

1
2
3 396 revealed a very similar isotopic enrichment of light Hg isotopes onto the surfaces. Based on these
4
5
6 397 laboratory studies we expect that light Hg isotopes are preferentially sequestered in soils and sediments
7
8 398 with enrichment factors in a relatively narrow range of about -0.3 ‰ to -0.6 ‰ in $\delta^{202}\text{Hg}$ for both thiol-
9
10 399 bound and mineral-bound Hg(II). As a consequence, the mobile phase, eventually leaching from soils
11
12 400 and sediments, is expected to be correspondingly enriched in heavy Hg isotopes. Furthermore, the
13
14
15 401 proposed enrichment of heavy Hg isotopes in the mobile Hg(II) pool should also be considered when
16
17 402 dealing with Hg isotope fractionation during bioaccumulation, as the mobile fraction is bioavailable.
18

19 403 20 21 22 404 **Acknowledgments**

23
24 405 We thank Kurt Barmettler for help in the soil chemistry lab, Felix Oberli for help with the Hg isotope
25
26 406 measurements, Robin S. Smith for various support, Felix Maurer for statistical advice, and three
27
28
29 407 anonymous reviewers for helpful comments. This research was funded by ETH Zurich (GrantNo. ETH-
30
31 408 15 09-2), which is gratefully acknowledged.
32

33 409 34 35 410 **Supporting Information**

36
37
38
39 411 Experimental details, statistical tests, additional figures, and data tables. This material is available free
40
41 412 of charge via the internet at <http://pubs.acs.org>.
42

43 44 413 **References**

- 45
46 414 (1) Selin, N. E., Global biogeochemical cycling of mercury: A review. *Annu. Rev. Environ. Resour.*
47
48 415 **2009**, *34*, 43-63.
49
50 416 (2) Skyllberg, U.; Westin, M. B.; Meili, M.; Bjorn, E., Elevated concentrations of methyl mercury in
51
52
53 417 streams after forest clear-cut: A consequence of mobilization from soil or new methylation? *Environ.*
54
55 418 *Sci. Technol.* **2009**, *43*, (22), 8535-8541.
56
57
58
59
60

- 1
2
3 419 (3) Skyllberg, U., Chemical Speciation of Mercury in Soil and Sediment. In *Environmental*
4
5 420 *Chemistry and Toxicology of Mercury*, Liu, G.; Cai, Y.; O'Driscoll, N. J., Eds. John Wiley & Sons, Inc.:
6
7
8 421 2011; pp 219-258.
- 9
10 422 (4) Gabriel, M. C.; Williamson, D. G., Principal biogeochemical factors affecting the speciation and
11
12 423 transport of mercury through the terrestrial environment. *Environ. Geochem. Health* **2004**, *26*, (4), 421-
13
14 424 434.
- 15
16
17 425 (5) Skyllberg, U., Mercury Biogeochemistry in Soils and Sediments. In *Synchrotron-based*
18
19 426 *Techniques in Soils and Sediments*, Singh, B.; Gräfe, M., Eds. Elsevier B.V.: Netherlands, 2010;
20
21 427 Developments in Soil Science; Vol. 34, pp 379-410.
- 22
23
24 428 (6) Kretzschmar, R.; Schäfer, T., Metal retention and transport on colloidal particles in the
25
26 429 environment. *Elements* **2005**, *1*, (4), 205-210.
- 27
28
29 430 (7) Bergquist, B. A.; Blum, J. D., The odds and evens of mercury isotopes: applications of mass-
30
31 431 dependent and mass-independent isotope fractionation. *Elements* **2009**, *5*, (6), 353-357.
- 32
33 432 (8) Blum, J. D., Applications of Stable Mercury Isotopes to Biogeochemistry. In *Handbook of*
34
35 433 *Environmental Isotope Geochemistry*, Baskaran, M., Ed. Springer Berlin Heidelberg: 2011; Advances
36
37 434 in Isotope Geochemistry; pp 229-245.
- 38
39
40 435 (9) Hintelmann, H.; Zheng, W., Tracking Geochemical Transformations and Transport of Mercury
41
42 436 through Isotope Fractionation. In *Environmental Chemistry and Toxicology of Mercury*, Liu, G.; Cai,
43
44 437 Y.; O'Driscoll, N. J., Eds. John Wiley & Sons, Inc.: 2011; pp 293-327.
- 45
46
47 438 (10) Schauble, E. A., Role of nuclear volume in driving equilibrium stable isotope fractionation of
48
49 439 mercury, thallium, and other very heavy elements. *Geochim. Cosmochim. Acta* **2007**, *71*, (9), 2170-
50
51 440 2189.
- 52
53
54 441 (11) Buchachenko, A. L., Mercury isotope effects in the environmental chemistry and biochemistry
55
56 442 of mercury-containing compounds. *Russ. Chem. Rev.* **2009**, *78*, (4), 319-328.
- 57
58
59 443 (12) Bergquist, B. A.; Blum, J. D., Mass-dependent and -independent fractionation of Hg isotopes by
60
444 photoreduction in aquatic systems. *Science* **2007**, *318*, (5849), 417-420.

- 1
2
3 445 (13) Zheng, W.; Hintelmann, H., Isotope fractionation of mercury during its photochemical reduction
4
5 446 by low-molecular-weight organic compounds. *J. Phys. Chem. A* **2010**, *114*, (12), 4246-4253.
6
7
8 447 (14) Rodriguez-Gonzalez, P.; Epov, V. N.; Bridou, R.; Tessier, E.; Guyoneaud, R.; Monperrus, M.;
9
10 448 Amouroux, D., Species-specific stable isotope fractionation of mercury during Hg(II) methylation by an
11
12 449 anaerobic bacteria (*Desulfobulbus propionicus*) under dark conditions. *Environ. Sci. Technol.* **2009**, *43*,
13
14
15 450 (24), 9183-9188.
16
17 451 (15) Malinovsky, D.; Vanhaecke, F., Mercury isotope fractionation during abiotic transmethylation
18
19 452 reactions. *International Journal of Mass Spectrometry* **2011**, *307*, (1-3), 214-224.
20
21
22 453 (16) Zheng, W.; Hintelmann, H., Nuclear field shift effect in isotope fractionation of mercury during
23
24 454 abiotic reduction in the absence of light. *J. Phys. Chem. A* **2010**, *114*, (12), 4238-4245.
25
26 455 (17) Kritee, K.; Blum, J. D.; Johnson, M. W.; Bergquist, B. A.; Barkay, T., Mercury stable isotope
27
28 456 fractionation during reduction of Hg(II) to Hg(0) by mercury resistant microorganisms. *Environ. Sci.*
29
30
31 457 *Technol.* **2007**, *41*, (6), 1889-1895.
32
33 458 (18) Malinovsky, D.; Latruwe, K.; Moens, L.; Vanhaecke, F., Experimental study of mass-
34
35 459 independence of Hg isotope fractionation during photodecomposition of dissolved methylmercury. *J.*
36
37
38 460 *Anal. At. Spectrom.* **2010**, *25*, (7), 950-956.
39
40 461 (19) Kritee, K.; Barkay, T.; Blum, J. D., Mass dependent stable isotope fractionation of mercury
41
42 462 during mer mediated microbial degradation of monomethylmercury. *Geochim. Cosmochim. Acta* **2009**,
43
44
45 463 *73*, (5), 1285-1296.
46
47 464 (20) Estrade, N.; Carignan, J.; Sonke, J. E.; Donard, O. F. X., Mercury isotope fractionation during
48
49 465 liquid-vapor evaporation experiments. *Geochim. Cosmochim. Acta* **2009**, *73*, (10), 2693-2711.
50
51
52 466 (21) Ghosh, S.; Schauble, E. A.; Lacrampe Couloume, G.; Blum, J. D.; Bergquist, B. A., Estimation
53
54 467 of nuclear volume dependent fractionation of mercury isotopes in equilibrium liquid-vapor evaporation
55
56 468 experiments. *Chem. Geol.* **in press**, (doi:10.1016/j.chemgeo.2012.01.008).
57
58
59 469 (22) Zheng, W.; Foucher, D.; Hintelmann, H., Mercury isotope fractionation during volatilization of
60
470 Hg(0) from solution into the gas phase. *J. Anal. At. Spectrom.* **2007**, *22*, (9), 1097-1104.

- 1
2
3 471 (23) Wiederhold, J. G.; Cramer, C. J.; Daniel, K.; Infante, I.; Bourdon, B.; Kretzschmar, R.,
4
5 472 Equilibrium mercury isotope fractionation between dissolved Hg(II) species and thiol-bound Hg.
6
7
8 473 *Environ. Sci. Technol.* **2010**, *44*, (11), 4191-4197.
9
10 474 (24) Pokrovsky, O. S.; Viers, J.; Emnova, E. E.; Kompantseva, E. I.; Freydier, R., Copper isotope
11
12 475 fractionation during its interaction with soil and aquatic microorganisms and metal oxy(hydr)oxides:
13
14
15 476 Possible structural control. *Geochim. Cosmochim. Acta* **2008**, *72*, (7), 1742-1757.
16
17 477 (25) Balistrieri, L. S.; Borrok, D. M.; Wanty, R. B.; Ridley, W. I., Fractionation of Cu and Zn
18
19 478 isotopes during adsorption onto amorphous Fe(III) oxyhydroxide: Experimental mixing of acid rock
20
21
22 479 drainage and ambient river water. *Geochim. Cosmochim. Acta* **2008**, *72*, (2), 311-328.
23
24 480 (26) Juillot, F.; Marechal, C.; Ponthieu, M.; Cacaly, S.; Morin, G.; Benedetti, M.; Hazemann, J. L.;
25
26 481 Proux, O.; Guyot, F., Zn isotopic fractionation caused by sorption on goethite and 2-lines ferrihydrite.
27
28 482 *Geochim. Cosmochim. Acta* **2008**, *72*, (19), 4886-4900.
29
30
31 483 (27) Mikutta, C.; Wiederhold, J. G.; Cirpka, O. A.; Hofstetter, T. B.; Bourdon, B.; Von Gunten, U.,
32
33 484 Iron isotope fractionation and atom exchange during sorption of ferrous iron to mineral surfaces.
34
35 485 *Geochim. Cosmochim. Acta* **2009**, *73*, (7), 1795-1812.
36
37
38 486 (28) Beard, B. L.; Handler, R. M.; Scherer, M. M.; Wu, L. L.; Czaja, A. D.; Heimann, A.; Johnson,
39
40 487 C. M., Iron isotope fractionation between aqueous ferrous iron and goethite. *Earth Planet. Sci. Lett.*
41
42 488 **2010**, *295*, (1-2), 241-250.
43
44
45 489 (29) Schauble, E. A.; Meheut, M.; Hill, P. S., Combining metal stable isotope fractionation theory
46
47 490 with experiments. *Elements* **2009**, *5*, (6), 369-374.
48
49 491 (30) Pokrovsky, O. S.; Viers, J.; Freydier, R., Zinc stable isotope fractionation during its adsorption
50
51 492 on oxides and hydroxides. *J. Colloid Interface Sci.* **2005**, *291*, (1), 192-200.
52
53
54 493 (31) Wasylenki, L. E.; Montanez, G.; Anbar, A. D. *Cd isotope fractionation during adsorption varies*
55
56 494 *with salinity* AGU, 90(52), Fall Meet. Suppl., San Francisco, 2009; Eos Trans.: San Francisco, 2009.
57
58 495 (32) Barling, J.; Anbar, A. D., Molybdenum isotope fractionation during adsorption by manganese
59
60 496 oxides. *Earth Planet. Sci. Lett.* **2004**, *217*, (3-4), 315-329.

- 1
2
3 497 (33) Brennecka, G. A.; Wasylenki, L. E.; Bargar, J. R.; Weyer, S.; Anbar, A. D., Uranium isotope
4
5 498 fractionation during adsorption to Mn-oxyhydroxides. *Environ. Sci. Technol.* **2011**, *45*, (4), 1370-1375.
6
7
8 499 (34) Siebert, C.; Nagler, T. F.; von Blanckenburg, F.; Kramers, J. D., Molybdenum isotope records as
9
10 500 a potential new proxy for paleoceanography. *Earth Planet. Sci. Lett.* **2003**, *211*, (1-2), 159-171.
11
12 501 (35) Weeks, C. L.; Anbar, A. D.; Wasylenki, L. E.; Spiro, T. G., Density functional theory analysis of
13
14 502 molybdenum isotope fractionation. *J. Phys. Chem. A* **2007**, *111*, (49), 12434-8.
15
16
17 503 (36) Wasylenki, L. E.; Weeks, C. L.; Bargar, J. R.; Spiro, T. G.; Hein, J. R.; Anbar, A. D., The
18
19 504 molecular mechanism of Mo isotope fractionation during adsorption to birnessite. *Geochim.*
20
21 505 *Cosmochim. Acta* **2011**, *75*, (17), 5019-5031.
22
23
24 506 (37) Cornell, R. M.; Schwertmann, U., Soils. In *The Iron Oxides*, Wiley-VCH Verlag GmbH & Co.
25
26 507 KGaA: 2004; pp 433-474.
27
28
29 508 (38) Forbes, E. A.; Posner, A. M.; Quirk, J. P., Specific adsorption of inorganic Hg(II) species and
30
31 509 Co(II) complex ions on goethite. *J. Colloid Interface Sci.* **1974**, *49*, (3), 403-409.
32
33 510 (39) Barrow, N. J.; Cox, V. C., The effects of pH and chloride concentration on mercury sorption. I.
34
35 511 By goethite. *J. Soil Sci.* **1992**, *43*, (2), 295-304.
36
37
38 512 (40) Kim, C. S.; Rytuba, J. J.; Brown, G. E., Jr., EXAFS study of mercury(II) sorption to Fe- and Al-
39
40 513 (hydr)oxides I. Effects of pH. *J. Colloid Interface Sci.* **2004**, *271*, (1), 1-15.
41
42 514 (41) Kim, C. S.; Rytuba, J.; Brown, G. E., Jr., EXAFS study of mercury(II) sorption to Fe- and Al-
43
44 515 (hydr)oxides - II. Effects of chloride and sulfate. *J. Colloid Interface Sci.* **2004**, *270*, (1), 9-20.
45
46
47 516 (42) Schwertmann, U.; Cornell, R. M., *Iron Oxides in the Laboratory - Preparation and*
48
49 517 *Characterisation*. Wiley-VCH: Weinheim, 2000; Vol. second edition.
50
51
52 518 (43) Reichard, P. U.; Kraemer, S. M.; Frazier, S. W.; Kretschmar, R., Goethite dissolution in the
53
54 519 presence of phytosiderophores: Rates, mechanisms, and the synergistic effect of oxalate. *Plant Soil*
55
56 520 **2005**, *276*, (1-2), 115-132.
57
58
59
60

- 1
2
3 521 (44) Wiederhold, J. G.; Kraemer, S. M.; Teutsch, N.; Borer, P. M.; Halliday, A. N.; Kretzschmar, R.,
4
5 522 Iron isotope fractionation during proton-promoted, ligand-controlled, and reductive dissolution of
6
7
8 523 goethite. *Environ. Sci. Technol.* **2006**, *40*, (12), 3787-3793.
9
10 524 (45) Powell, K. J.; Brown, P. L.; Byrne, R. H.; Gajda, T.; Hefter, G.; Sjöberg, S.; Wanner, H.,
11
12 525 Chemical speciation of Hg(II) with environmental inorganic ligands. *Aust. J. Chem.* **2004**, *57*, (10), 993-
13
14 526 1000.
15
16
17 527 (46) Blum, J.; Bergquist, B., Reporting of variations in the natural isotopic composition of mercury.
18
19 528 *Anal. Bioanal. Chem.* **2007**, *388*, (2), 353-359.
20
21
22 529 (47) Coplen, T. B., Guidelines and recommended terms for expression of stable-isotope-ratio and
23
24 530 gas-ratio measurement results. *Rapid Commun. Mass Spectrom.* **2011**, *25*, (17), 2538-2560.
25
26 531 (48) Mathur, S. S.; Dzombak, D. A., Chapter 16 Surface complexation modeling: goethite. In
27
28 532 *Interface Science and Technology*, Lützenkirchen, J., Ed. Elsevier: 2006; Vol. Volume 11, pp 443-468.
29
30
31 533 (49) Fischer, L.; Brümmer, G. W.; Barrow, N. J., Observations and modelling of the reactions of 10
32
33 534 metals with goethite: adsorption and diffusion processes. *Eur. J. Soil Sci.* **2007**, *58*, (6), 1304-1315.
34
35 535 (50) Collins, C. R.; Sherman, D. M.; Ragnarsdottir, K. V., Surface complexation of Hg²⁺ on goethite:
36
37 536 Mechanism from EXAFS spectroscopy and density functional calculations. *J. Colloid Interface Sci.*
38
39 537 **1999**, *219*, (2), 345-350.
40
41
42 538 (51) Sarkar, D.; Essington, M. E.; Misra, K. C., Adsorption of mercury(II) by variable charge
43
44 539 surfaces of quartz and gibbsite. *Soil Sci. Soc. Am. J.* **1999**, *63*, (6), 1626-1636.
45
46
47 540 (52) Dzombak, D. A.; Morel, F. M., *Surface complexation modeling: hydrous ferric oxide*. Wiley:
48
49 541 New York, 1990.
50
51
52 542 (53) Gustafsson, J. P. *Visual MINTEQ 3.0*, KTH (Royal Institute of Technology): Sweden, 2011.
53
54 543 (54) Wilkins, R. G., *Kinetics and Mechanism of Reactions of Transition Metal Complexes*. 2nd ed.;
55
56 544 Wiley-VCH Verlag 2003.
57
58
59
60

- 1
2
3 545 (55) Fricke, G.; Heilig, K., 80-Hg Mercury. In *Landolt-Boernstein. Numerical Data and Functional*
4
5 546 *Relationships in Science and Technology. Group 1. Elementary Particles, Nuclei and Atoms*, Springer:
6
7 Heidelberg, 2004; Vol. 20.
8
9
10 548 (56) Gunneriusson, L.; Sjöberg, S., Surface complexation in the H⁺-goethite ([alpha]-FeOOH)-Hg
11
12 549 (II)-chloride system. *J. Colloid Interface Sci.* **1993**, *156*, (1), 121-128.
13
14
15 550 (57) Barrow, N. J.; Gerth, J.; Brümmer, G. W., Reaction kinetics of the adsorption and desorption of
16
17 551 nickel, zinc and cadmium by goethite. II Modelling the extent and rate of reaction. *J. Soil Sci.* **1989**, *40*,
18
19 552 (2), 437-450.
20
21
22 553 (58) Fujii, T.; Moynier, F.; Dauphas, N.; Abe, M., Theoretical and experimental investigation of
23
24 554 nickel isotopic fractionation in species relevant to modern and ancient oceans. *Geochim. Cosmochim.*
25
26 555 *Acta* **2011**, *75*, (2), 469-482.
27
28
29 556 (59) Black, J. R.; Kavner, A.; Schauble, E. A., Calculation of equilibrium stable isotope partition
30
31 557 function ratios for aqueous zinc complexes and metallic zinc. *Geochim. Cosmochim. Acta* **2011**, *75*, (3),
32
33 558 769-783.
34
35 559 (60) Fujii, T.; Moynier, F.; Telouk, P.; Abe, M., Experimental and theoretical investigation of isotope
36
37 560 fractionation of zinc between aqua, chloro, and macrocyclic complexes. *J. Phys. Chem. A* **2010**, *114*,
38
39 561 (7), 2543-2552.
40
41
42 562 (61) Gehrke, G. E.; Blum, J. D.; Slotton, D. G.; Greenfield, B. K., Mercury isotopes link mercury in
43
44 563 San Francisco bay forage fish to surface sediments. *Environ. Sci. Technol.* **2011**, *45*, (4), 1264-1270.
45
46
47 564 (62) Yin, R.; Feng, X.; Wang, J.; Bao, Z.; Yu, B.; Chen, J., Mercury isotope variations between
48
49 565 bioavailable mercury fractions and total mercury in mercury contaminated soil in Wanshan Mercury
50
51 566 Mine, SW China. *Chem. Geol.* **in press** (doi: 10.1016/j.chemgeo.2012.04.017).
52
53
54 567
55
56 568
57
58
59
60